Original Research Article

The Combined Effect of Nanoclay and α-tocopherol on Mechanical and Physical Properties of Polyethylene Active Packaging

Zahra Mirkhavar[1], Shervin Ahmadi[2], Mehdi Farhoodi[1], Abdorreza Mohammadi[1], Mohammad Amin Mohammadifar[1,3,*]

[1]Department of Food Science and Technology, Faculty of Nutrition Science, Food Science and Technology/National Nutrition and Food Technology Research Institute, Shahid Beheshti University of Medical Sciences, Tehran, IRAN.
[2]Department of Polymer Processing, Iran Polymer and Petrochemical Institute, Tehran, IRAN.
[3]Research Group for Food Production Engineering, National Food Institute, Technical University of Denmark, SøltoftsPlads, 2800 Kongens Lyngby, DENMARK.

Submission Date: 15-06-2018; Revision Date: 26-07-2018; Accepted Date: 30-08-2018

ABSTRACT

A novel active nanocomposite packaging based on low-density polyethylene (LDPE), Cloisite® 15 A (C15A), and α -tocopherol (α-TOC) was prepared. The effects of C15A (0-4 wt. %) and α-TOC (1-3 wt. %) on optical, mechanical and barrier properties of polyethylene were analyzed using the Response Surface Methodology (RSM). Regression models were developed for mechanical characteristics (tensile strength and elongation at break), water vapor permeability (WVP) and optical properties (L*, a*, b*, OP) as a function of α-TOC and C15A concentrations. For all cases, the quadratic terms of the model were significant ($P< 0.05$). In order to maximize TS and EL and minimize WVP, the desirability function (DF) was used to determine the regression model equations. The optimized factors were found to be 2.93 wt. % α-TOC and 4 wt.% Cloisite®15A for a maximal desirability of 0.903.

Key words: Active packaging, α-tocopherol, Cloisite®15A, Nanocomposite, RSM.

Correspondence:
Mohammad Amin Mohammadifar,
Research Group for Food Production Engineering, National Food Institute, Technical University of Denmark, SøltoftsPlads, 2800 Kongens Lyngby, DENMARK.

Email: moamo@food.dtu.dk

INTRODUCTION

Oils and fat oxidation is one of the major chemical deterioration modes limiting the shelf life of fatty foods during the storage time[1] Antioxidants are extensively incorporated into foods for preventing oxidation and extending the shelf life. Adding antioxidants to foods includes two methods of direct addition of antioxidant into foods or the indirect method using packaging.[2] Antioxidant packaging has been investigated for a very long time, as a method to inhibit oxidation and preserve food quality and nutrition by their controlled release.[3-4]

SCAN QR CODE TO VIEW ONLINE

www.ajbls.com

DOI : 10.5530/ajbls.2018.7.5

Another significant finding was that incorporating the antioxidant into a food package protects the degradation of polymers during processing.[5-6] Consumer demand for natural food products has derived in an increased attention in using natural active components such as plant extracts and α –tocopherol.[6-7]

Alpha-tocopherol is a biological antioxidant.[8] Natural tocopherol has been widely used in the structure of various polymeric films like LDPE and polypropylene because it was resistant under high-temperature process, represent good solvability in the polyolefin, to protect the polymer while producing less off-flavor and improve the sensory quality of food.[9] Antioxidants are sensitive to heat. The low molecular weight of polyethylene makes it appropriate as a matrix for natural antioxidant active packaging. Polyethylene is one of the most widely used polyolefins in the packaging industry for food packaging due to its attractive combination of a low density, low production cost, chemical inertness, acceptable heat

distortion temperature and easy processability.[10] The incorporation of antioxidants in packaging matrix may change the mechanical and optical properties of film and decrease gas barrier. To solve these problems, adding the appropriate type of reinforcement such as nanoclay is the efficient method to improve packaging properties. In addition, Nanoclay can help the release of active compounds for a longer time by increasing their solvability in the nanocomposite resulting in the protection of foods for an extended period.[11] Montmorillonite is the most widely used layered silicates in industrial applications due to its large aspect ratio and high surface area.[12-13] Such Clays are immiscible with hydrophobic polymers because of its hydrophilic characteristic. In order to improve miscibility with other polymer matrices, modifying the nanoclay surface seems necessary. The modified layered silicates are known as organoclays such as closite15A.[14-15]

In this study, α -tocopherol as an antioxidant, closite 15A as a nano filler and polyethylene as a polymer matrix, was used to fabricate a new antioxidant nanocomposite via melt extrusion. In order to determine the optimal nanocomposite formulation, response surface methodology was used. RSM is a multivariate analysis designing the experimental conditions, creating the models with the best conditions, reducing the number of experimental runs, Request permission estimating the effects of factors and identifying the possible interactions.[16]

The objective of this study was to evaluate the effects of α-TOC and C15A on the mechanical, optical and gas barrier properties of the fabricated nanocomposite.

MATERIALS AND METHODS

Material

Low density polyethylene resin (density = 0.92 gml^{-1}, MFI = 2 g/10 min) and high-density polyethylene resin (density = 0.952 gml^{-1}, MFI=18 g/10min) were provided from Amir Kabir Petrochemical Co. (Tehran, Iran). Organically-modified montmorillonite (OMM) nanomer, Cloisite® 15 A (C15A), was purchased from Southern Clay Products Company (USA). α -tocopherol was provided from Sigma Aldrich. (Germany) at ≥ 96% purity.

Statistical analysis and experimental design

The experiments were performed based on the faced center (CCD) combined with RSM. Faced center (CCD) provides us with the opportunity of using Duncan's Test to determine the significant differences in response. The statistical software Design-Expert 7.0.0 (Stat-Ease Inc., Minneapolis) was applied for creating the design matrix and analyzing the experimental data. The input parameters, i.e. α-TOC and C15A, were coded at three levels (- 1, 0, +1). Based on the Central composite design (CCD), 13 experiments including five center points were used with α -tocopherol concentration (X_1, wt. %) (1, 2, 3) while C15A concentration (X_2, wt. %) (0, 2, 4) was the independent process variable.

The amounts of α-TOC and C15A were presented in (Table 1). All the experimental tests were performed in triplicate followed by Duncan's Test and the mean of the results was used for RSM. Mean values were compared by Analysis of Variance (ANOVA) using SPSS 19.0.0 (IBM, Chicago IL, USA). The statistical significance was defined as $P < 0.05$.

A polynomial mathematical model was used to correlate the association between the dependent (Y) and the independent (X_1 and X_2) variables as expressed by the following equation:

$$Y = \beta_0 + \sum_{i=1}^{k} \beta_i X_i + \sum_{i=1}^{k} \beta_{ii} X_i^2 + \sum_{\substack{i=1 \\ i<j}}^{k-1} \sum_{j=2}^{k} \beta_{ij} X_i X_j$$

Where Y represents the response; Xi and X j represent the variables; β0 indicates the constant term and βi indicates the coefficient of the polynomial for linear effect; βii show quadratic coefficients and and βij represents interaction coefficients and k represents the number of studied parameters.

Nanocomposite fabrication

For preparing samples, first, LDPE and HDPE in a weight ratio of 85 to 15 were premixed and used as a based polymer. Polyethylene and C15A were dried in a vacuum oven (90°C for 48 h). Based on the design experiment results, PE, C15A and α-TOC were manually mixed (Table 1). A twin/screw extruder (L/D=40, D=25 mm, ZSK 25 gravimetric fed) and a temperature profile of 150, 155, 150, 165, 170 and 175°C were employed for film production. After the extrusion process, the samples were pelletized and then the pellets were dried at 40°C under vacuum for 24 h. Then, the pellets were shaped as films by a Brabender DCE 330single-screw extruder (L= 400 mm and L/D= 20) and blown film unit. The constant temperature profile of 190°C was employed for film production. Extrusion parameters such as temperature profile and feeding rate were optimized by preliminary works. The films were cooled on a chill roll.

Film thickness

The film thickness, considered as the average of ten random locations, was measured with the digital micrometer (Elcometer, United Kingdom).

Film tensile properties

The tensile test was conducted based on the ASTM D638 standard on dumbbell-shaped specimens (Standard). Dumbbells were made by injection molding machine and conditioned at 55% relative. The samples were tensioned on a tensile tester (SANTAM, STM50) with speed test = 5 mm/min and load cell = 5000 N at room temperature. The stress-strain curves were plotted while tensile strength (TS) and elongation at break (%EB) of the specimens were calculated as follows:

$$TS\ (MPa) = F_{max}\ (N)\ /A_{min}\ (m^2) \times 10^{-6}$$

$$EB\ (\%) = L_{max}\ (m)\ /L_0\ (m) \times 100$$

F_{max} represents maximum load, A_{min} represents the minimum cross section area, L_{max} represents an extension at the moment of rupture and L_0 represents the initial length of the sample.

Water vapor permeability (WVP)

In order to calculate the WVP of the film specimen, first, the Water Vapor Transmission Rate (WVTR) of the specimen was determined at 30ºC and 75% RH conditions based on the standard method E96, with some modifications.[17] The films were cut into 4 cm diameter circles and mounted directly on the top of WVP cups containing anhydrous calcium chloride as a drying agent. The cups were located in a climate chamber at the controlled temperature. The weight of the cups was measured until the equilibrium weight was reached. WVTR was determined from the slope of mass changes against time achieved with a linear regression. By multiplying the thickness of the film in the WVTR and dividing it by the difference in pressure between the relative humidity of the tubes and desiccator, the permeability to the water vapor was obtained. The WVTR and WVP can be measured as follows:

$$WVTR = S/A$$

$$WVP = (X\ (m) \times WVTR/3600\ \Delta P\ (Pa))$$

Where S represents Curve slope (gr/s), A represents the Film area (m^2), X represents thickness (m) and ΔP represents Pressure difference (3,185 (Pa))

Color measurement

The color of samples was measured by Chroma meter (Color Flex EZ, Spectrophotometers, Hunter Lab and USA). The L*, a* and b* of the measurements were presented where L* shows the lightness, with a range from 0 to 100 (black, white); a * shows redness, from green (-) to red (+); b * shows yellowness, from blue (-) to yellow (+). Opacity values (%) were measured based on the Hunterlab method using the same tool of color evaluation. The opacity percentage of the specimen was determined with reflectance measurements of each sample with standard black and white backing plates based on the following equation:

$$Opacity = Y1/Y2$$

Where Y1and Y2 represent the CIE tristimulus value of the sample with the black and white backing plates respectively.[18]

Confirmation and optimization procedures

The numerical optimizations were applied by Design-Expert 7.0.0 software. In order to determine the optimum percentage of α-TOC and C15A to predict the best value of mechanical and WVP responses, graphical and numerical optimization procedures were applied. Parameter levels and the corresponding response value were optimized and a verification test was applied using the predicted parameters.

RESULT AND DISCUSSION

Analysis of regression models

The samples were provided based on the software proposed values for the α-TOC wt. % and C15A wt. % (Table 1). The considered responses including mechanical properties (TS, EL), gas barrier properties (WVP) and optical properties (L*, a*, b*, OP) were measured and analyzed with software.

Table 1: Experimental design used for α-TOC and C15A based nanocomposites and the coded and actual Variables for the CCD.

Treatment	Coded Variable		Actual Variable	
	X1	X2	α- TOC (wt %)	C15A (wt %)
1	-1	-1	1	0
2	1	-1	3	0
3	-1	1	1	4
4	1	1	3	4
5	-1	0	1	2
6	1	0	3	2
7	0	-1	2	0
8	0	1	2	4
9	0	0	2	2
10	0	0	2	2
11	0	0	2	2
12	0	0	2	2
13	0	0	2	2

Table 2: The related equations between the considered responses extracted from the software.

Response	Equation*	R^2	Adj-R^2	Pred-R^2	C.V. %
TS	$=11.65 -0.18X_1+0.42X_2+0.15X_1X_2+0.25X_1^2+0.19X_2^2$	0.9753	0.9577	0.8482	0.67
EL	$= 117.08 + 9.65\ X_1+ 3.33\ X_2 + 3.51\ X_1\ X_2 - 9.12\ X_1^2$	0.9867	0.9801	0.9302	1.12
WVP	$= 2.76 -2.27\ X_1 - 1.867\ X_2 + 2.88\ X_1\ X_2+1.48\ X_2^2$	0.9899	0.9849	0.9459	9.93
L*	$=80.48-0.47X_1-0.46X_2+0.84X_1X_2-0.62X_1^2-0.52X_2^2$	0.9916	0.9855	0.9508	0.13
a*	$=1.95-0.040X_1-0.18X_2-0.065X_1X_2+0.12X_1^2+0.35X_2^2$	0.9952	0.9917	0.989	1.34
b*	$= 5.43 + 1.39\ X_1+ 2.44\ X_2 - 0.83\ X_1\ X_2 - 0.75\ X_2^2$	0.9868	0.9802	0.9368	5.8
OP	$= 5.10 - 0.14\ X_1 - 0.033\ X_2 - 0.075\ X_1\ X_2 +0.060\ X_2^2$	0.9723	0.9585	0.9172	0.46

To find the best regression equations, experiment data were fit through different models (linear, quadratic, interactive and cubic). To checking the adequacy of models, the sequential sum of squares and model summary statistics were used. The sequential sum of squares indicated that, for all cases, the quadratic model was suggested (p-value < 0.01).

Lack of Fit test was performed on the empirical data to compare the consistency of the model. The quadratic model indicated the insignificant lack of fit.[19] Unaccounted systematic Varian in the hypothesized model could explain significant lack of fit. Small variations in the independent variables of the model could also lead to such results.[20] The R^2 range as a critical factor to check model achieved in this study showed the suitability of the experimental data as R^2 close to 100% confirms the validity of the model. Similarly, maximum adjusted form of R^2 (adj-R^2) for a number of terms in the model indicates the suitability of the model. Model summary statistics indicated that for all cases the quadratic model had maximum adjusted R-squared and predicted R-squared and minimum standard deviation (SD) values (Table 2).

To find the statistical significance of the regression coefficient and its parameters, Analysis of Variance was performed. The term coefficients which are found statistically insignificant should be eliminated from the model.[21] The F-tests revealed a high model F-values and low p-values (P < 0.001) indicating that the factor had a significant impact on the response. Based on ANOVA in case of TS, L*and a*, the p-values for all terms of the model was significant (P < 0.001), while in case of EL, the quadratic effect of C15A concentration (X_2^2) was insignificant (PV=0.3693) and removed from the model. In the case of WVP, b * and OP, the p-values of the quadratic effect of α-TOC concentration (X_1^2) was insignificant. Thus, the modified equation was extracted by removing these terms. The high values of R^2 (>0.97 %), R^2 Adj (>0.95 %) and R^2 Pred (>0.84 %), for all cases, indicated that the model had the great predictive ability. In this research, the coefficient of variation (CV) was less than 10% for all cases.[22]

After analyzing the correlated mathematical equations in the coded form, the relationship between the examined properties and the controlling parameters were obtained (Table 2).

Interactive effects of nanoparticles on mechanical properties

The regression equations, in terms of the coded factor, indicated that the linear effect of α-TOC concentration (X_1) was the most significant factors associated with EL model while the effect of α-TOC was greater than C15A concentration (X_2) and their interaction (X_1X_2) effect. For TS, the linear effect of closite-15A concentration (X_2), the quadratic effect of α-TOC and C15A concentration (X_1^2, X_2^2) and interaction effect of them (X_1X_2) was positive while the linear effect of α-TOC concentration(X_1) was negative factors associated with TS (Table 2).

To visualize the interactions between the factors and the answers (TS, EL), 3D surfaces were used as a function of closite-15A and α-TOC (Figure 1). Significant interaction effects existed among the factors (closite-15A wt. % and α-TOC wt. %) indicating quadratic effects on TS and EL. At all levels of α-TOC, TS increased by increasing C15A wt. %. Such an improvement in the TS of nanocomposite may be indicated the uniform disper-

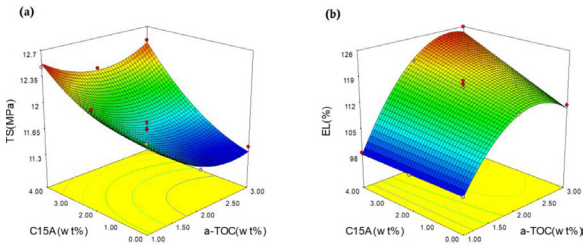

Figure 1: Profile of response surface plot for TS (a) and EL (b), as function of α-TOC and C15A nanoparticles concentrations (wt%).

Table 3: Mechanical and WVP properties of α-TOC/PE/C15A nanocomposites (Means±SD*).

Run	Sample	TS (MPa)	EL (%)	WVP ($g^1m^{-1}.Pa^{-1}.S^{-1}$) ($\times10^{-12}$)
1	1α-TOC/0C15A	11.97 ± 0.09^{aA}	98.37 ± 5.28^{aA}	11.55 ± 1.09^{cC}
5	1α-TOC/2C15A	12.14 ± 0.20^{bB}	98.02 ± 6.21^{aA}	$4.69\pm.61^{bC}$
3	1α-TOC/4C15A	12.48 ± 0.11^{cB}	98.57 ± 7.50^{aA}	$2.13\pm.32^{aA}$
7	2α-TOC/0C15A	11.37 ± 0.08^{aA}	113.71 ± 6.97^{aB}	$6.00\pm.74^{bB}$
9	2α-TOC/2C15A	11.65 ± 0.40^{aA}	116.13 ± 3.10^{aB}	$3.13\pm.28^{aB}$
8	2α-TOC/4C15A	12.28 ± 0.12^{bA}	119.27 ± 8.49^{aBC}	$2.12\pm.09^{aA}$
2	3α-TOC/0C15A	11.41 ± 0.33^{aA}	111.65 ± 6.68^{aB}	0.80 ± 0.05^{aA}
6	3α-TOC/2C15A	11.63 ± 0.55^{aA}	115.32 ± 5.64^{aB}	$1.01\pm.10^{aA}$
4	3α-TOC/4C15A	12.5 ± 0.34^{bB}	125.88 ± 4.11^{bC}	$2.9\pm.19^{bA}$

The small letters are used for comparison the samples with the same α -tocopherol content and capital letters are used for samples with the same Closite 15A content. The same letters shows the mean values that are not significantly different ($P>0.05$). *SD: Standard Deviation

sion of C15A in the polymer matrix and strong interaction between PE and nanoclay. At all concentrations of C15A, the increase in α-tocopherol content resulted in the decrease of tensile strength which can explain that the stronger interactions of PE intermolecular were partially replaced by weaker PE and α-tocopherol interactions in the film matrix.[23-24]

On the other hand, an increasing of α-TOC content resulted in increases elongation at break. α- tocopherol is an oily compound acting as a lubricant in the PE structure and promoting the chain sliding during the extension.[25]

Based on Duncan test, the increase of C15A concentration had insignificant effects on EL at low and medium concentrations of α-tocopherol while the increment of C15A concentration significantly increased the EL of specimens at high concentrations of a-tocopherol (Table 3). Chemical compatibility among the polymer and the filler plays an important role in the dispersion of nanoclay within the matrix and in the adhesion between C15A and PE and the modified polymers have the higher elongation at break compared to the neat polymer. Coupling agents are used for improving the intercalation of nanocomposites due to increasing the interlayer distance of nanoclays, which can cause to improve the penetration of the polymer into clay galleries and indicates better-exfoliated structure and better mechanical characteristics than the polymer without coupling agent.[26]

Interactive effects of nanoparticles on Water vapor permeability (WVP)

The regression equations indicated that X_1 and X_2 had a negative effect while X_1X_2 and X_2^2 had a positive effect on Water Vapor Permeability (Table 2). The WVP of the nanocomposite films was measured and showed in (Table 3). Significant interaction effects existed between α -TOC and C15A concentrations indicating the quadratic effects on WVP. The response surface of the WVP of the nanocomposites as a function of α -TOC and C15A content is presented in (Figure 2). Based on WVP test results, increasing in α -tocopherol content resulted in the decrease in WVP at low and medium concentrations of C15A, while the effect of α-tocopherol in high concentrations of nanoparticles on decreasing WVP was not significant. This was possibly caused by an increase in the films' hydrophobicity in the presence of α-tocopherol. Adding hydrophobic components into a polymeric matrix could generate a barrier effect on the transmission of water molecules if they were homogeneously scattered in the film.[27] Similar conclusions were observed in LDPE film with α-tocopherol,[28] starch-sodium caseinate films containing α –tocopherol[29] PVA film incorporated with clove oil[24] and PVA film incorporated with green tea extract.[30] In the case of nanoclay, the increase of C15A wt. %

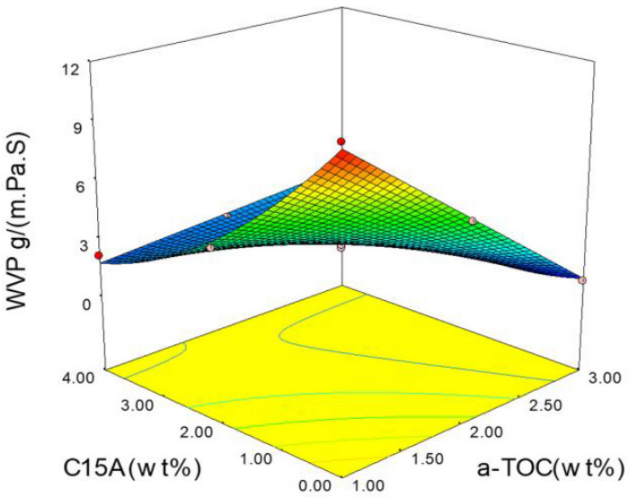

Figure 2: Profile of response surface plot for WVP as function of α-TOC and C15A nanoparticles concentrations (wt%).

reduced water vapor permeability values. According to Nielsen theory, the uniform distribution of clay layers in the matrix of polymer increases the diffusion path of gas and provides excellent barrier properties. In general, the diffusion of gases in the nanocomposite depends on a number of factors including aspect ratio, volume fraction and above all, the degree of exfoliation in the polymer nanocomposite.[26]

Interactive effects of nanoparticles on optical properties

The color properties of films play a significant role in the appearance of packaging and consumer acceptability.[31] The regression equations indicated that the interactive effect of α-TOC and nanoclay concentration (X_1X_2) was the most significant factor related to L* while the main and quadratic X_1 and X_2 had the negative and X_1X_2 had the positive effect on lightness index. For a* index, the quadratic effect of (X_2^2) was the most significant model parameter. The nanoclay concentration was the most significant variable affecting b*. Finally, the main effect of α-TOC was the most significant variable affecting OP and only X_2^2 had a positive effect on OP (Table 2).

In order to show the relationship effect of factors, i.e., nanoclay and α-TOC concentrations on color properties (L*, a*, b*) and OP, the 3D response surface plot were introduced as the function of two variables concentrations (Figure 3). By increasing of C15A and α-TOC, the L* value decreases, while the L* value increases at high levels of α-TOC by increasing C15A (Figure 3a), similarly, a decrease in L* value with addition of nanoclays[32] was already reported in the literature.

Based on the Duncan test (Table 4), increasing of α-TOC had an insignificant effect on a* value at all level of C15A. At all levels of α-TOC, a* reduced initially by increasing closite.15A concentration and then increased (Figure 3b).

As indicated in Figure 3c, b* value, increased by increasing C15A and α-TOC concentration at all levels. The films containing antioxidants and nanoclay indicated higher b* values with increasing concentration of α-TOC[5,33] and nanoclay.[34] Differences in rolls film were perceptible to the eye.

As indicated in Figure 3d, OP value, decreased by increasing α-TOC concentration at all levels. Based on the results presented in Table 4, the effect of C15A concentration on OP was insignificant at low and medium concentrations of α-tocopherol while this factor had a significant effect on the OP at the high level of α-TOC. On the other hand, the decrease of OP by increasing α-TOC was significant at all level of C15A concentration.

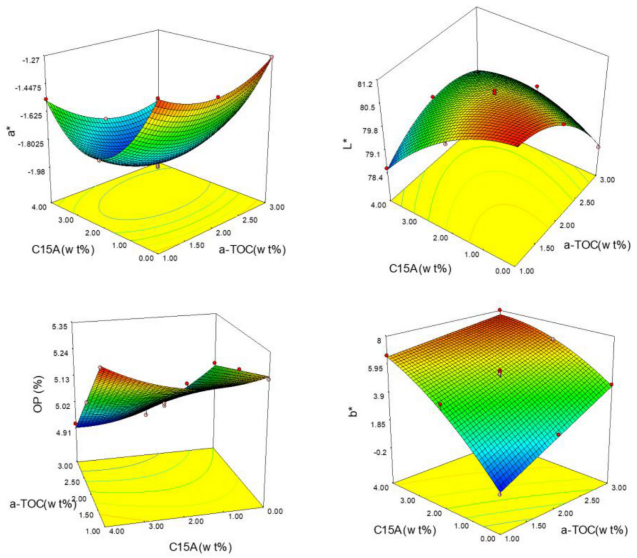

Figure 3: Profile of response surface plot for a) L* b) a* c) b* and d) OP as function of α-TOC and C15A nanoparticles concentrations (wt%).

Table 4: Color and opacity parameters of α-TOC/ PE/C15A nanocomposites (Means±SD*).

Run	Sample	L*	a*	b*	OP(%)
1	1α-TOC/0C15A	81.16 ± 0.11^{cC}	-1.32 ± 0.02^{cB}	-0.16 ± 0.01^{aA}	5.35 ± 0.02^{aB}
5	1α-TOC/2C15A	80.25 ± 0.09^{bB}	-1.8 ± 0.04^{aB}	4.45 ± 0.39^{bA}	5.26 ± 0.03^{aC}
3	1α-TOC/4C15A	78.55 ± 0.16^{aA}	-1.54 ± 0.05^{bB}	6.62 ± 0.32^{cA}	5.34 ± 0.02^{aC}
7	2α-TOC/0C15A	80.43 ± 0.19^{bB}	-1.42 ± 0.03^{cA}	2.33 ± 0.20^{aB}	5.20 ± 0.07^{aA}
9	2α-TOC/2C15A	80.46 ± 0.11^{bC}	-1.98 ± 0.02^{aA}	5.49 ± 0.06^{bB}	5.08 ± 0.06^{aB}
8	2α-TOC/4C15A	79.54 ± 0.28^{aB}	-1.78 ± 0.03^{bA}	6.72 ± 0.32^{cA}	5.12 ± 0.03^{aB}
2	3α-TOC/0C15A	78.43 ± 0.30^{aA}	-1.28 ± 0.03^{cB}	4.53 ± 0.79^{aC}	5.14 ± 0.04^{bA}
6	3α-TOC/2C15A	79.52 ± 0.27^{cA}	-1.86 ± 0.01^{aB}	6.74 ± 0.24^{bC}	4.94 ± 0.04^{aA}
4	3α-TOC/4C15A	79.19 ± 0.25^{bB}	-1.76 ± 0.05^{bA}	8.00 ± 0.57^{cB}	4.93 ± 0.04^{aA}

Small letters are used for comparison the means of samples with the same α -tocopherol content and capital letters are used for the same Closite 15A content. The same letters shows the mean values that are not significantly different ($P>0.05$). *SD: Standard Deviation

Table 5: Predicted and Confirmation value for the responses at optimum point.

Responses	Predicted value	Confirmation value
TS (MPa)	12.44	12.73
EL (%)	124.76	126.1
WVP ($g^{1}m^{-1}.Pa^{-1}.S^{-1}$)	$2.94^{\times}\ 10^{-12}$	$2.65^{\times}10^{-12}$

Optimization of multiple responses

In order to optimize the nanocomposite films and determine the optimal amount of α -tocopherol and nanoclay, the numerical optimization method was used. In response surface methodology, desirability function approach was the most used in multi-response optimization.[35] For each response, a DF approach assigns numbers between 0 (undesirable) and 1(desirable) response value. The individual desirability was incorporated into a single function resulting in the overall desirability. Depending on the response to be maximized, minimized or made equal to the target value, different desirability functions can be used.[36]

The analysis of responses of the TS, EL and WVP described as response surface optimization. The desired target for α-tocopherol and C15A concentrations variables were selected in the range, while the TS and SB were set to maximum and the minimum was applied for WVP. Based on the software suggestion, the optimized factors were 2.93 % TOC and 4% nanoclay for highest value desirability of 0.903. The individual desirability indicated that the settings were more effective at maximizing the TS (0.948) and EL (0.96) than minimizing WVP (0.80). The maximum desirability value of d= 0.903 shows the suitability of the design for use.

To validate the adequacy of the model equations, a confirmation experiment was performed with optimal variable concentrations. The TS, EL and WVP values from the confirmation experiment were relevant closely related to the obtained data from desirability optimization by RSM, as shown in Table 5.

CONCLUSION

The present study aimed at using the RSM for modeling the effects of α-TOC and C15A on mechanical, gas barrier and optical properties of α-TOC /PE/ C15A nanocomposites as summarized below. The results of the analysis of variance indicated that the two parameters, i.e. α-TOC and C15A, can act as efficient variables on the TS, EL, WVP and optical properties of nanocomposites. Adding nanoclay (C15A) improved the tensile strength and gas barrier properties of nanocomposites while showing an insignificant effect on elongation at break. Alpha-tocopherol with polar "head" structure and the linear "tail" can act as a coupling agent to improve the mechanical and WVP due to increased interaction between fillers and matrix. Desirability function was employed for the multi response optimization. The optimized parameters for maximum TS and EL and minimum WVP were predicted as 2.93 wt.%- α-TOC and 4 wt.% C15A. The results obtained from the confirmation experimental response values were in accordance with the predicted values.

ACKNOWLEDGEMENT

We are grateful for the financial support from the National Nutrition and Food Technology Research Institute of Iran.

CONFLICT OF INTEREST

The authors declare no conflict of interest.

ABBREVIATIONS USED

LDPE: low-density polyethylene; **C15A:** Cloisite®15A; **α-TOC:** α -tocopherol; **RSM:** Response Surface Methodology; **TS:** Tensile Strength; **EL:** Elongation at Break; **WVP:** Water Vapor Permeability; **OP:** Optical Properties; **DF:** Desirability Function.

REFERENCES

1. Labuza TP, Dugan JL. Kinetics of lipid oxidation in foods. Critical Reviews in Food Science and Nutrition. 1971;2(3):355-405.
2. Shen L, Chen X, Lee DS, Zhu X, Chen M, Yam KL. Effects of diffusion controlled release of tocopherol on lipid oxidation. Food Packaging and Shelf Life. 2018;17:129-33.
3. López-de-Dicastillo C, Gómez-Estaca J, Catalá R, Gavara R, Hernández-Muñoz P. Active antioxidant packaging films: development and effect on lipid stability of brined sardines. Food Chemistry. 2012;131(4):1376-84.
4. Sun LN, Lu LX, Qiu XL, Tang YL. Development of low-density polyethylene antioxidant active films containing α-tocopherol loaded with MCM-41 (Mobil Composition of Matter No. 41) *Mesoporous silica*. Food Control. 2017;71:193-9.
5. Manzanarez-López F, Soto-Valdez H, Auras R, Peralta E. Release of α-Tocopherol from Poly(lactic acid) films and its effect on the oxidative stability of soybean oil. Journal of Food Engineering. 2011;104(4):508-17.
6. Ramos M, Beltrán A, Peltzer M, Valente AJM, Garrigós MdC. Release and antioxidant activity of carvacrol and thymol from polypropylene active packaging films. LWT - Food Science and Technology. 2014;58(2):470-7.
7. Barbosa-Pereira L, Cruz JM, Sendón R, de Quirós ARB, Ares A, Castro-López M, *et al*. Development of antioxidant active films containing tocopherols to extend the shelf life of fish. Food Control. 2013;31(1):236-43.
8. Shankar S, Rhim JW. Tocopherol-mediated synthesis of silver nanoparticles and preparation of antimicrobial PBAT/silver nanoparticles composite films. LWT - Food Science and Technology. 2016;72:149-56.
9. Koontz JL. Chapter 13 - Packaging Technologies to Control Lipid Oxidation. In: Hu M, Jacobsen C, editors. Oxidative Stability and Shelf Life of Foods Containing Oils and Fats: AOCS Press. 2016;479-517.
10. Ahmed J, Arfat YA, Al-Attar H, Auras R, Ejaz M. Rheological, structural, ultraviolet protection and oxygen barrier properties of linear low- density

polyethylene films reinforced with zinc oxide (ZnO) nanoparticles. Food Packaging and Shelf Life. 2017;13:20-6.
11. Sanchez-Garcia M, Gimenez E, Lagaron J. Morphology and barrier properties of solvent cast composites of thermoplastic biopolymers and purified cellulose fibers. Carbohydrate Polymers. 2008;71(2):235-44.
12. Nasiri A, Peyron S, Gastaldi E, Gontard N. Effect of nanoclay on the transfer properties of immanent additives in food packages. Journal of Materials Science. 2016;51(21):9732-48.
13. Xue Y, Shen M, Lu F, Han Y, Zeng S, Chen S, *et al*. Effects of heterionic montmorillonites on flame resistances of polystyrene nanocomposites and the flame retardant mechanism. 2017.
14. Babu VR, Loganathan S, Pugazhenthi G, Thomas S, Varghese TO. Chapter 2 - An Overview of Polymer–Clay Nanocomposites. In: Jlassi K, Chehimi MM, Thomas S, editors. Clay-Polymer Nanocomposites: Elsevier. 2017;29-81.
15. Kotal M, Bhowmick AK. Polymer nanocomposites from modified clays: Recent advances and challenges. Progress in Polymer Science. 2015;51:127-87.
16. S Araújo C, Rodrigues AMC, Joele R, Araújo EAF, Lourenço LFH. Optmizing process parameters to obtain a bioplastic using proteins from fish byproducts through the response surface methodology. Food Packing and Shelf Life. 2018;16:23-30.
17. Intl A. Standard test method for water vapor transmission of materials. E 96-00. Annual book of ASTM standards Philadelphia, Pa: ASTM Intl p. 2000;307-14.
18. Teixeira B, Marques A, Pires C, Ramos C, Batista I, Saraiva JA, *et al*. Characterization of fish protein films incorporated with essential oils of clove, garlic and origanum: Physical, antioxidant and antibacterial properties. LWT-Food Science and Technology. 2014;59(1):533-9.
19. Sun G, Zhang X, Bao Z, Lang X, Zhou Z, Li Y, *et al*. Reinforcement of thermoplastic chitosan hydrogel using chitin whiskers optimized with response surface methodology. Carbohydrate Polymers. 2018;189:280-8.
20. Cao J, Wu Y, Jin Y, Yilihan P, Huang W. Response surface methodology approach for optimization of the removal of chromium(VI) by NH2-MCM-41. Journal of the Taiwan Institute of Chemical Engineers. 2014;45(3):860-8.
21. Mäkelä M. Experimental design and response surface methodology in energy applications: A tutorial review. Energy Conversion and Management. 2017;151:630-40.
22. Koocheki A, Taherian AR, Razavi SMA, Bostan A. Response surface methodology for optimization of extraction yield, viscosity, hue and emulsion stability of mucilage extracted from Lepidium perfoliatum seeds. Food Hydrocolloids. 2009;23(8):2369-79.
23. Atarés L, Chiralt A. Essential oils as additives in biodegradable films and coatings for active food packaging. Trends in Food Science and Technology. 2016;48:51-62.
24. Chen C, Xu Z, Ma Y, Liu J, Zhang Q, Tang Z, *et al*. Properties, vapour-phase antimicrobial and antioxidant activities of active poly (vinyl alcohol) packaging films incorporated with clove oil. Food Control. 2018;88:105-12.
25. Sin LT, Bee ST, Tee TT, Kadhum AAH, Ma C, Rahmat A, *et al*. Characterization of α-tocopherol as interacting agent in polyvinyl alcohol–starch blends. Carbohydrate Polymers. 2013;98(2):1281-7.
26. Azeredo HMCD. Nanocomposites for food packaging applications. Food Research International. 2009;42(9):1240-53.
27. Anbinder PS, Peruzzo PJ, Amalvy JI. Effect of food additives on the microstructure, mechanical and water transport properties of polyurethane films. Progress in Organic Coatings. 2016;101:207-15.
28. Sun LN, Lu LX, Qiu XL, Tang YL. Development of low-density polyethylene antioxidant active films containing α-tocopherol loaded with MCM-41 (Mobil Composition of Matter No. 41) *Mesoporous silica*. Food Control. 2017;71:193-9.
29. Jiménez A, Fabra MJ, Talens P, Chiralt A. Physical properties and antioxidant capacity of starch–sodium caseinate films containing lipids. Journal of Food Engineering. 2013;116(3):695-702.
30. Chen CW, Xie J, Yang FX, Zhang HL, Xu ZW, Liu JL, *et al*. Development of moisture-absorbing and antioxidant active packaging film based on poly (vinyl alcohol) incorporated with green tea extract and its effect on the quality of dried eel. Journal of Food Processing and Preservation. 2018;42(1):e13374.
31. Abdollahi M, Rezaei M, Farzi G. A novel active bionanocomposite film incorporating rosemary essential oil and nanoclay into chitosan. Journal of Food Engineering. 2012;111(2):343-50.
32. Abolghasemi FL, Ghanbarzadeh B, Dehghannya J, Abbasi F, Ranjbar H. Optimization of mechanical and color properties of polystyrene/nanoclay/nano ZnO based nanocomposite packaging sheet using response surface methodology. Food Packaging and Shelf Life. 2018;17:11-24.
33. Marcos B, Sárraga C, Castellari M, Kappen F, Schennink G, Arnau J. Development of biodegradable films with antioxidant properties based on polyesters containing α-tocopherol and olive leaf extract for food packaging applications. Food Packaging and Shelf Life. 2014;1(2):140-50.
34. Tornuk F, Sagdic O, Hancer M, Yetim H. Development of LLDPE based active nanocomposite films with nanoclays impregnated with volatile compounds. Food Research International. 2018;107:337-45.
35. Morshedi A, Akbarian M. Application of response surface methodology: design of experiments and optimization: a mini review. J Fund Appl Life Sci. 2014;54:2434-9.
36. Figueroa RAR, Cassano A, Drioli E. Ultrafiltration of orange press liquor: optimization for permeate flux and fouling index by response surface methodology. Separation and Purification Technology. 2011;80(1):1-10.

Cite this article: Mirkhavar Z, Ahmadi S, Farhoodi M, Mohammadi A, Mohammadifar MA. The Combined Effect of Nanoclay and α-tocopherol on Mechanical and Physical Properties of Polyethylene Active Packaging. Asian J Biol Life Sci. 2018;7(2):59-66.